Synthesis and characterization of polyurethanes with high renewable carbon content and tailored properties

Tamara Calvo-Correas[1], M. Dolores Martin[2], Aloña Retegi[1], Nagore Gabilondo[1], Maria Angeles Corcuera[1], Arantxa Eceiza[1]*

[1] *Group 'Materials + Technologies', Department of Chemical and Environmental Engineering, Faculty of Engineering of Gipuzkoa, University of the Basque Country, Pza Europa 1, Donostia-San Sebastian, 20018, Spain*

[2] *Macrobehavior-Mesostructure-Nanotechnology General Research Service (SGIker) Faculty of Engineering of Gipuzkoa, University of the Basque Country, Plaza Europa 1, 20018 Donostia-San Sebastian, Spain*

**corresponding author: arantxa.eceiza@ehu.eus*

Telephone number: +34 943017185

ABSTRACT

Thermoplastic and crosslinked biobased polyurethanes with a renewable carbon content ranging from 78 to 98% were synthesized and characterized. The macrodiol and the diisocyanate used were derived from renewable source, the first one from castor oil, and the second one from fatty acid. Moreover, the chain extenders employed were derived from corn sugar and polysaccharides. The effect of component molar ratios and chain extender and crosslinker structure in final properties was analyzed. Thermal analysis revealed that polyurethanes are formed by amorphous and crystalline domains. It was also observed that the crystallinity of the material is related with components molar ratio and also with their structure. Besides, mechanical properties and morphology were tightly dependent on the overall crystallinity, allowing the synthesis of biobased polyurethanes with tailored properties and high renewable carbon content.

Keywords: fatty acid derived diisocyanate, biobased polyurethane, structure/properties relationship, amorphous domains, crystalline domains.

INTRODUCTION

Segmented polyurethanes (STPU) are one of the most employed polymers due to their versatility regarding properties ranging from elastomers to rigid, which make possible their use in multiple applications. These polymers are usually constituted of two segments; one formed by a macrodiol, commonly a polyether or polyester type diol, and the other is a urethane type segment usually obtained by the reaction of a diisocyanate and a low molecular weight chain extender. The thermodynamic incompatibility between both segments leads to microphase separation, which is strongly dependent on chemical structure and block lengths, as well as it is influenced by factors

such as hydrogen bonding and crystallization extent [1–6]. That is why structure and nature of the starting materials have a key role on the behavior and the final properties of the material.

Furthermore, the demand for the design of polyurethanes derived from renewable sources has increased due to the depletion of the world crude oil stock and economical, environmental and social concerns [7–9]. In the last decades, the use of macrodiols derived from vegetable oils, such as castor, rapeseed and linseed oil, has been widely studied for the synthesis of biobased polyurethanes [10,11]. Over the past few years, different vegetable oils derived macrodiols have been proved competitive for the synthesis of a wide range of polyurethanes [5,12–16]. However, although the most employed diisocyanates for the synthesis of polyurethanes are derived from petroleum, it is noteworthy the increased use of biobased diisocyanates. One of the most studied is L-lysine diisocyanate (LDI), which is derived from L-lysine amino acid [17–20]. Nevertheless, recently is gaining attention the employ of fatty acids-based diisocyanates such as dimeryldiisocyanate (DDI) [21–23]. The use of this kind of diisocyanates with a non symmetrical chemical structure results in the formation of amorphous urethane based domains with low glass transition temperature. Therefore, polyurethanes with a segment formed by this kind of diisocyanate and a segment formed by a macrodiol with a melting temperature much higher than room temperature, results in STPUs showing a different behavior comparing with common polyurethanes [24].

In this work thermoplastic and crosslinked biobased polyurethanes were synthesized, in both cases a macrodiol derived from castor oil and dimer fatty acid-based diisocyanate were employed. On the one hand, for the synthesis of thermoplastic biobased polyurethanes two different chain extenders were used: 1,3- propanediol, based on corn sugar, and dianhydro-D-glucitol, also known as isosorbide, which is obtained from polysaccharides. On the other hand, the biobased crosslinked polyurethane was obtained employing 1,1,1-tris(hydroxymethyl)propane crosslinker. Both, the thermoplastic and the crosslinked polyurethanes were synthesized in bulk varying the molar ratio of the components and without using any chemical catalysts.

This work is aimed at studying the effects of the chain extender or crosslinker structure and component molar ratios on the final properties of biobased polyurethanes. Thermal properties were measured by means of differential scanning calorimetry (DSC) and dynamic mechanical analysis (DMA). Physicochemical and mechanical properties were analyzed using Fourier transform infrared spectroscopy (FTIR), gel permeation chromatography (GPC) and performing tensile and Shore D hardness tests, respectively. The morphology of the synthesized biobased polyurethanes was also analyzed by atomic force microscopy (AFM). Finally, surface properties were analyzed by measuring water contact angle (WCA).

EXPERIMENTAL

Materials

Poly(butylene sebacate)diol derived from castor oil was used in the synthesis of the biobased polyurethanes. This macrodiol has a hydroxyl index of 32.01 mgKOH g^{-1} determined by titration with ASTM D 4274-88 Method A and a number-average molecular weight of 3505 g mol^{-1}, which was characterized in a previous work [5]. Furthermore, as diisocyanate 2-heptyl-3,4-bis(9-isocyanatononyl)-1-pentylcyclohexane (DDI) (587 g mol^{-1} and an isocyanate content of 13.6-14.3 %) was used, supplied by GL Syntech (USA). Two biobased chain extenders were employed, 1,3 propanediol (PD) (76 g mol^{-1}) based on corn sugar and dianhydro-D-glucitol (DAS) (146 g mol^{-1}) derived from polysaccharides, supplied by Quimidroga and Sigma-Aldrich, respectively. 1,1,1-Tris(hydroxymethyl)propane (TMP) (134.17 g mol^{-1}) was used as crosslinker, which was supplied by Fluka. The biobased carbon content of the starting materials was determined by ASTM-D6866-12 (0.98) Method B (AMS) standard procedure. The macrodiol has a 72 %, DDI has a 98 %, and PD and DAS have a 100 % of biobased carbon content. All starting materials were used as received, except macrodiol and PD, which were previously dried under vacuum for 6 h at 80 and 40 ºC, respectively. The chemical structures of the starting materials employed are shown in Figure 1.

Synthesis of the biobased polyurethanes

Two-step bulk polymerization procedure was used for the synthesis of biobased polyurethanes without using any catalyst. The reaction was carried out in a 250 mL five-necked round-bottom flask equipped with a mechanical stirrer and dry nitrogen inlet. First, dried macrodiol and diisocyanate were placed in the flask and heated in a thermo-regulated silicon bath at 80 ºC for 4 h to obtain the prepolymer. The reaction mixture was homogeneous. Then, the chain extender or the crosslinker was added to the prepolymer at 80 ºC and the mixture was rapidly stirred for 10-15 min. Finally, the resulting viscous liquid was quickly poured between two Teflon® coated metal plates heated at 100 ºC and separated by 1.5 mm. Several compression-decompression cycles were applied in order to remove the air bubbles and then pressed at the same temperature under 50 bar for 10 h. The NCO to OH groups molar ratio for all biobased thermoplastic and crosslinked polyurethanes was kept constant at 1.01. The synthesized polyurethanes, their molar ratio, DDI/chain extender or crosslinker content and biobased carbon content are gathered in Table 1. Samples have been designated as PUx-y where x is the abbreviation of the chain extender or crosslinker and y is DDI/chain extender or crosslinker content calculated as weight percentage of DDI and chain extender or crosslinker respect to total biobased polyurethane weight. As a reference pure DDI/PD, DDI/DAS and DDI/TMP segments (PUPD-100, PUDAS-100 and PUTMP-100, respectively) were also synthesized. The biobased carbon content in the

polyurethanes was estimated having into account the molar ratio and the biobased carbon content of each component in the final formulation (Table 1).

Characterization techniques

Weight average molecular weight, $\overline{M}_w$, and dispersity index (PI) of the synthesized biopolyurethanes were determined by GPC using a Thermo Scientific chromatograph, equipped with an isocratic Dionex UltiMate 3000 pump and a RefractoMax 521 refractive index detector. The separation was carried out at 30 ºC within four Phenogel GPC columns from Phenomenex, with 5 µm particle size and 10^5, 10^3, 100 and 50 Å porosities, respectively, located in an UltiMate 3000 Thermostated Colum Compartment. Tetrahydrofuran (THF) was used as mobile phase at a flow rate of 1 mL min^{-1}. Samples were prepared dissolving the obtained biopolyurethanes in THF at 1 wt% and filtering using nylon filters with 2 µm pore size. $\overline{M}_w$ and PI were reported as weight average polystyrene standards.

The identification of biobased polyurethane characteristic functional groups and hydrogen-bonding interactions was performed by FTIR using a Nicolet Nexus FTIR spectrometer equipment with a MKII Golden Gate accessory with diamond crystal at a nominal incident angle of 45º and a ZnSe lens. The spectra were obtained after 32 scans in a range from 4000 to 800 cm^{-1} with a resolution of 4 cm^{-1}.

Thermal properties were investigated by means of DSC using a Mettler Toledo DSC822e equipment. Samples with a weight between 5 and 10 mg were sealed in aluminum pans and heated from -70 to 150 ºC at a scanning rate of 20 ºC min^{-1}, using N_2 as a purge gas (20 mL min^{-1}). The crystallization process was also followed by cooling the samples from 150 to -70 ºC at scanning rate of 5 ºC min^{-1}. A second heating was run at the same conditions of the first heating, being this the reported result. The inflexion point of the heat capacity change observed was chosen to evaluate glass transition temperature, T_g. Melting temperature (T_m) was settled as the maximum of endothermic peak taking the area under the peak as melting enthalpy (ΔH_m). Crystallization temperature (T_c) was taken as the minimum of the exothermic peak observed in the cooling scan and the crystallization enthalpy (ΔH_c) as the peak area.

The dynamic mechanical behavior of the biobased polyurethanes was analyzed by DMA in tensile mode on an Eplexor 100N analyzer from Gabo, using a static strain of 0.10%. The temperature was varied from -100 to 100 ºC at a scanning rate of 2 ºC min^{-1} and at a fixed operation frequency of 10 Hz. Samples were cut in strips of 22 mm in length, 5 mm in width and 1.5 mm in thickness. Moreover, crosslink density (ν_e) and molecular weight between crosslinks ($\overline{M}_c$) [25,26] values of the crosslinked biobased polyurethane were determined by equations 1 and 2 respectively.

$$\nu_e = \frac{E'}{3RT} \qquad (1)$$

$$\bar{M}_c = \frac{\rho}{\nu_e} \qquad (2)$$

where E' is the storage modulus at temperature above T (in the rubbery region at T_g + 85 ºC), R is the universal constant of gases (8.314 J mol^{-1} K^{-1}), T is temperature in Kelvin and ρ is the density of the biobased polyurethane (1.2 g cm^{-3}).

Mechanical testing was carried out at room temperature using a Universal Testing Machine (MTS Insight 10) with a load cell of 10 kN and pneumatic grips. Samples were cut into dog-bone shape according to ASTM D1708-93 standard procedure. Tests were performed with a crosshead rate of 50 mm min^{-1}. Elastic modulus (E), tensile strength at break (σ) and percentage elongation at break (ε) were averaged from at least five test specimen data.

Shore D hardness measurements were performed at room temperature with a MD-202 DuroTECH digital hardness testing device following ASTM D2240 standard procedure. Results were also averaged from a least five values measured in different zones of the sample.

AFM was used to characterize biobased polyurethanes morphology by imaging the cross-sections of the samples cut with a Leica EM FC6 cryo-ultramicrotome equipped with a diamond knife at -140 ºC. This temperature was chosen in order to attempt to cut the samples in the glassy state, to obtain an adequate surface. Images were obtained in tapping mode at room temperature with a Bruker Dimension ICON scanning probe microscope equipped with a Nanoscope V Controller. Samples morphology was examined using TESP-V2 type silicon tips having a nominal resonance frequency of 320 kHz and a cantilever spring constant about 42 N m^{-1}.

The surface properties of synthesized biobased polyurethanes were evaluated measuring the water contact angle (WCA) in Dataphysics OCA20 equipment. Five measurements of each sample were carried out with a deionised water drop method (2 μL) at 26 °C. The surface tension between the surface of the material and water was calculated using Neumann's Equation of State (3), which is based on the equilibrium of forces at the edge of a resting drop, as proposed by Young.

$$\gamma_{PU} = \frac{1}{4}\gamma_{H_2O}\,(1+\cos\beta)^2 \qquad (3)$$

where γ_{PU} is the surface tension of the biopolyurethane, γ_{H_2O} is the water surface tension and β is the angle between water drop and biobased polyurethane surface.

RESULTS AND DISCUSSION

Since polymer properties are strongly dependent on their molecular weight, average molecular weight and dispersity index of the synthesized biobased thermoplastic polyurethanes have been measured and the values are gathered in Table 1. It can be seen that $\overline{M}_w$ for both systems are similar, and the slightly higher values determined for PUDAS biopolyurethanes could be attributed to a higher molar mass of DAS. In the same way, $\overline{M}_w$ shows in both systems a decreasing trend with the increase of DDI/chain extender content, which could be attributed to the higher amount of DDI and chain extender [27]. In any case, the variations on the molecular weight can be ascribed to segment architecture [28].

FTIR was used in order to analyze the characteristic groups of the biobased polyurethanes. All the compositions show a similar behavior, however for the sake of higher clarity only the infrared spectra of PUPD-48, PUDAS-50 and PUPTMP-49 as well as pure macrodiol and neat DDI spectra are shown in Figure 2. The isocyanate group stretching band was not found at 2270 cm^{-1}, indicating that complete polymerization has occurred. Therefore the free catalyst employed synthesis method was suitable. The synthesized biobased polyurethanes show a band around 3365 cm^{-1} associated to the N-H stretching vibration of urethane group [17] and at 1530 cm^{-1} a band ascribed to C-N stretching vibration combined to N-H out-of-plane bending [12]. Furthermore, the carbonyl group stretching region is shown in the inset, where the macrodiol presents a band at 1726 cm^{-1} associated to carbonyl stretching in ester group [24]. It is well know that the infrared absorbance of C=O and N-H groups in polyurethanes shifts to different wavenumbers depending if they are free or H-bonded [6,29]. As can be observed the synthesized biobased polyurethanes show a broad band at 1728 cm^{-1}, which encompasses the infrared absorbance of C=O group of the macrodiol and the free urethane C=O group. Regarding to the urethane H-bonded C=O group, PUPD-48 and PUDAS-50 present a peak at 1689 and 1692 cm^{-1}, respectively. The peak is more intense in PUPD-48 according to a lower steric hindrance due to its linear structure, which allows an easier chain association by H-bonding. In this way, PUTMP-49 polyurethane has a lower ability to associate properly due to its crosslinked structure and that is why a shoulder appears between 1680 and 1713 cm^{-1}. In the same way, the peak ascribed to N-H stretching vibration of urethane group appears at lower wavenumber according to a higher association by H-bonding, being PUPD biobased polyurethane the one which shows the lowest wavenumber value, followed by PUDAS and PUTMP, corroborating the behavior observed in the carbonyl group stretching region.

DSC was used in order to characterize the thermal behavior. Figure 3 shows the DSC thermograms for the synthesized biobased polyurethane series together with macrodiol and neat DDI/chain extender or crosslinker. The thermal transitions are listed in Table 3. The semicrystalline macrodiol shows a T_g at -52 ºC and an endothermic peak associated with crystals melting at 70 ºC. Regarding neat DDI/chain extender biobased polyurethanes, PUPD-100 shows

a T_g around -14 ºC and two endothermic peaks at 45 and 60 ºC respectively, while neat PUDAS-100, besides the T_g at -1 ºC, shows an endothermic peak at higher temperature than PUPD-100, at 89 ºC, due to its bicyclic structure. However, PUTMP-100 shows a T_g at higher temperature than T_g of PUPD-100 and PUDAS-100, around 9 ºC, since net points hinder chains mobility resulting in a higher T_g [30]. In the same way, PUTMP-100 is not able to crystallize owing to the formation of a crosslinked structure inhibits chains motion for crystallization [31,32]. The use of DDI as diisocyanate results in polyurethanes with low T_g and T_m, due to its branched aliphatic structure hinders the association by hydrogen bonding and leads to flexible chains. In previous works [24,33] thermoresponsive biobased polyurethanes were synthesized using ethyl ester L-lysine diisocyanate (LDI) as diisocyanate, as well as the same macrodiol, PD and TMP employed in this work. Similarly to DDI the side chain of the aliphatic LDI inhibited the crystallization of neat LDI/PD and LDI/TMP biopolyurethanes. However, since LDI molecule is smaller, the resultant chains were stiffer and T_g values of 33 and 59 ºC, respectively, were obtained. Nevertheless, the thermal behavior of DDI differs from the reported in the literature when classical diisocyanates like aromatic 4,4'-diphenylmethane diisocyanate (MDI) or aliphatic 1,6-hexametylene diisocyanate (HDI) are employed. For instance, Cognet-Georjon et al. [34] reported a stiff polyurethane formed by MDI/DAS with a T_g of 187 ºC and a T_m of 235 ºC. In the same way, Saralegi et al. [5] synthesized a HDI/PD polyurethane with a T_g of 60 ºC and a T_m higher than 160 ºC.

Regarding synthesized biobased polyurethanes with different macrodiol/DDI/chain extender or crosslinker content, all of them present several thermal transitions related to those observed for neat blocks. At low temperatures, PUPD and PUDAS biobased polyurethanes show a T_g which slightly increases as DDI/PD and DDI/DAS contents increase, while in PUTMP biobased polyurethanes is practically constant. The T_g is an indicator of the relative purity of the phases. The miscibility between domains depends on their respective lengths, affinity between them and also to the ability of segments to crystallize [1,5,35]. Due to the chemical structure of DDI a fraction of DDI/chain extender is mixed with the amorphous macrodiol. In this way as DDI chain extender content increases T_g also increases according to the miscibility between blocks. For PUPD series the T_g values are slightly higher due to the lower steric hindrance of the linear PD allows a higher miscibility. Similar behavior was observed in the polyurethanes synthesized with LDI [24,33], as LDI/PD or TMP content increased T_g also slightly increased according to a higher miscibility of the amorphous LDI with the amorphous phase of the macrodiol. In contrast, different behaviors where observed when more classical diisocyanates are used. Cognet-Georjon et al. [35] reported a polyurethane system containing a 35 and 48 wt % of MDI/DAS segment and a polyether polyol (2000 g mol^{-1} molecular weight), with a T_g slightly higher than the T_g of neat polyol (11-13 ºC), almost independent to hard segment content. This slight increase was attributed

to restrictions of the mobility of soft segments and not to dissolved hard segment [36,37]. Moreover, Saralegi et al. [5] synthesized a polyurethane with HDI and the same biobased macrodiol and PD used in this work. They found T_g values around -50 ºC, which were also independent to hard segment content and showed a higher degree of phase separation. Similarly, when the trans-trans isomer content of 4,4'-dicyclohexyl methane diisocyanate (H_{12}MDI) was increased from 45 to 98 % (determined by ^{13}C NMR) [38], a decrease in T_g was observed and becomes closer to macrodiol T_g, suggesting an increase in the soft segment purity and hence the formation of ordered hard domains which contributed to a better phase separation. Moreover, in PUPD polyurethanes, between 30 and 70 ºC, an endothermic peak with a shoulder can be seen. As mentioned before, PUPD-100 show two peaks at similar temperatures meaning that the endothermic peak observed encompasses the melting enthalpy of both, macrodiol and DDI/PD rich domains. However, as DDI/PD content increases the enthalpy of the peak (58 ºC) decreases, while the shoulder at 45 ºC increases becoming a peak. Therefore, the peak could be mainly associated with the microdomain formed by macrodiol and the shoulder with the one formed by DDI/PD. Regarding, PUDAS and PUTMP polyurethanes, as DDI/DAS or DDI/TMP content increases the endothermic peak observed decreases, according to a lower content of macrodiol rich microdomain. Nevertheless, as DDI/DAS content increases a second endothermic peak appears around 75 ºC, which could be associated with the melting of crystals formed by DDI/DAS rich microdomain. Melting enthalpy values for PUPD biopolyurethanes are higher than the ones of PUDAS and PUTMP polyurethanes according to PD is a linear small molecule with a lower steric hindrance, which facilitates the efficient packaging of macrodiol chains to form crystals and also due to the contribution of the melting of DDI/PD crystals. Furthermore, the cooling scans (inset on the left of each figure) show a similar behavior, where as DDI/chain extender or crosslinker content increases crystallization temperature and enthalpy also decrease.

The dynamic mechanical behavior of the synthesized polyurethanes was analyzed by means of DMA. The temperature dependence of the storage modulus (E') and loss factor (tanδ) for the synthesized biobased polyurethanes is shown in Figure 4 and the glass transition temperatures are gathered in Table 3. It was observed a similar behavior for all the synthesized biobased polyurethanes. As macrodiol content increases the storage modulus values in the glassy state is slightly higher, according to a higher crystallinity [32]. At higher temperatures, the materials show a decrease in E' associated with the glass transition temperature. In addition, after the decrease of E', biobased polyurethanes reach a plateau, where E' value decreases with the increase of DDI/chain extender or crosslinker content, due to less ordered domains corresponding to semicrystalline macrodiol, which provide significant structural reinforcement [5,32]. In the same way, E' values are higher for PUPD biobased polyurethanes according to a higher crystallinity of the material, which is in accordance with the results obtained by DSC and FTIR. Finally, at higher

temperature E' decreases due to the disruption of ordered domains formed by the macrodiol. For PUDAS-50 the E' decrease is less abrupt due to the crystals formed by DDI/DAS domain which show higher T_m, as it was seen by DSC, which contributes also to the physical crosslink. PUTMP crosslinked polyurethane does not flow after the disruption of crystalline macrodiol domains. The material reaches a second plateau, where the storage modulus value increases with the increase of DDI/TMP rich domain content, suggesting a more crosslinked structure. Crosslink density (ν_e) and average molecular weight between crosslinks ($\overline{M}_c$) values were estimate in order to quantify the crosslink degree (values are gathered in Table 2). As can be observed the increase of DDI/TMP content increases crosslink densities of the biobased polyurethanes, meaning that net points are closer to each other decreasing $\overline{M}_c$. Nevertheless, PUTMP-27 shows considerably low crosslink density, and hence high $\overline{M}_c$ value, this fact could be due to the amount of crosslink agent is not high enough to build a crosslinked structure with net points close to each other. Regarding tanδ curve a wide peak with a maximum can be observed, which is mainly related with the mechanical transition (α) of the DDI/chain extender or crosslinker rich domain [35], since increases in intensity and temperature as DDI/chain extender or crosslinker rich domain content increases. In addition, this wide peak also encompasses the transition related with macrodiol rich domain. PUDAS and PUTMP biobased polyurethanes show higher α transition temperature than PUPD according to a higher steric hindrance of DAS and TMP which inhibits the mobility of the chains.

The strain-stress curves are shown in Figure 5 and the values derived from them together hardness Shore D values are gathered in Table 4. For all systems, storage modulus and stress at break increases as macrodiol content increases due to the higher crystallinity of the material which acts as a reinforcement [19]. Similar trend was also observed in other biopolyurethanes synthesized with the same macrodiol used in this works and amorphous urethane rich domains like LDI/PD [24], where it was seen that mechanical properties were mainly governed by the crystallizable macrodiol rich domain. However, when crystallizable urethane rich domains like HDI/PD [5] were used, also with the same macrodiol, stress at break and storage modulus increased as HDI/PD increased, contributing both domains to the observed improvement.

Regarding elongation at break of the synthesized STPUs, PUPD-36 and PUDAS-37 show a significant increase on the elongation. This fact could be related to the formation of crystals composed by DDI/PD and DDI/DAS segments which could be able to absorb more strain energy upon deformation, acting as effective stress-bearing phase during deformation [21,39]. However, for PUPD-48 and PUDAS-50 samples the formation of crystals formed by longer DDI/PD and DDI/DAS segments could contribute to the appearance of more breaking points which result in a steep decrease in elongation, being more pronounced in PUDAS-50, in agreement with the results

obtained by DSC and DMA. Regarding elongation at break of PUTMP system, it decreases as DDI/TMP content increases, according to the restrictions of net points. Regarding hardness of the synthesized materials, as DDI/chain extender or crosslinker content increase hardness values decrease according to a lower crystallinity of the material. However, PUDAS-50 shows a higher value. This fact might be due to the presence of DDI/DAS crystals, which have a higher T_m than macrodiol crystals, providing the material a higher hardness. Similar behavior was found in literature for amorphous rich domains, as well as for crystallizable rich domains [5,24].

In order to a deeper understanding of the final properties of the synthesized materials, the morphology was analyzed by AFM (Figure 6). As can be observed all the biobased polyurethanes present a microstructure where different domains can be distinguished. The lighter regions correspond to the crystalline domains and the darker ones to amorphous domains. These dark regions increase as DDI/chain extender or crosslinker content increases, according to a lower overall crystallinity of the material. Regarding the morphology of PUPD-36 and PUDAS-37, it seems more homogeneous and could be the reason of the greater deformability observed for these materials. However, an orientation in the morphology can be observed, especially in PUPD36, which could take place during the cryo-cut of the samples due to their higher ductility as also observed in mechanical testing.

Contact angle and surface tension values are gathered in Table 5. Since fatty acid groups have hydrophobic properties [40], the contact angle of all the synthesized biobased polyurethanes increases in general as DDI/chain extender or crosslinker content increases. In the same way, the surface tension of the materials decreases as DDI/chain extender or crosslinker content increases. Comparing PUPD and PUDAS biobased polyurethanes similar values were observed at each DDI/chain extender content, suggesting that the contact angle is more influenced by the amount of fatty acid groups instead of the structure of the chain extender. Nevertheless, PUTMP biobased polyurethane show a higher hydrophobicity according to its crosslinked structure [41].

CONCLUSIONS

Thermoplastic and crosslinked biobased polyurethanes with high biobased carbon content were synthesized successfully by a catalyst free two step bulk polymerization process using a macrodiol based on castor oil and a diisocyanate on fatty acids. In the case of thermoplastic polyurethanes the chain extenders employed were derived from corn sugar and polysaccharides, while the crosslinker used in the crosslinked biobased polyurethane was derived from petrochemical sources.

It was seen that the use of DDI as diisocyanate results in polyurethanes with low T_g and its branched structure inhibits the crystallization. As DDI/chain extender or crosslinker content

increases the T_g slightly increased, denoting a mixing of DDI/chain extender or crosslinker with the amorphous phase of the macrodiol. The influence of the structure of the chain extender or crosslinker was also seen, as their steric hindrance increased higher T_g values and lower ability to crystallize were observed. Moreover, an inversion of the behavior of the segments was observed, since the T_m of the crystallizable phase of the macrodiol was higher than the T_g, which made the macrodiol to act as hard segment. These results differed with the observed in the literature when conventional diisocyanates are employed, where segments with high T_g and T_m are obtained. The mechanical properties were tightly dependent on the overall crystallinity and morphology. As the crystallinity of the material increased mechanical properties improved, which allows the possibility of synthesizing biobased polyurethanes with tailored mechanical properties. Furthermore, the different behavior observed for the synthesized biobased polyurethanes in comparison with the results available in literature allows a deeper understanding of the chemistry of polyurethane synthesis.

ACKNOWLEGMENTS

Financial support from the Basque Government (IT-776-13) and from the Spanish Ministry of Economy and Competitiveness (MINECO) (MAT2013-43076-R) is gratefully acknowledged. We also wish to acknowledge the "Macrobehavior-Mesostructure-Nanotechnology" SGIker unit from the University of the Basque Country, for their technical support. T.C-C. thanks the University of the Basque Country for Ph.D. grant (PIF/UPV/12/200).

REFERENCES

[1] Petrovic, Z. S.; Javni, I.; Effect of soft-segment length and concentration on phase separation in segmented polyurethanes. J. Polym. Sci. Part B Polym. Phys. **1989**, 27, 545–560.

[2] Leung, L. M.; Koberstein, J. T. DSC annealing study of microphase separation and multiple endothermic behavior in polyether-based polyurethane block copolymers. Macromolecules **1986**, 19, 706–713.

[3] Castro, J. M.; Lopez-Serrano, F.; Camargo, R. E.; Macosko, C. W.; Tirrell, M. Onset of phase separation in segmented urethane polymerization. J. Appl. Polym. Sci. **1981**, 26, 2067–2076.

[4] Wang, C. S.; Kenney, D. J. Effect of hard segments on morphology and properties of thermoplastic polyurethanes. J. Elastomers Plast. **1995**, 27, 182–199.

[5] Saralegi, A.; Rueda, L.; Fernández-d'Arlas, B.; Mondragon, I.; Eceiza, A.; Corcuera, M. A. Thermoplastic polyurethanes from renewable resources: effect of soft segment

chemical structure and molecular weight on morphology and final properties. Polym. Int. **2013**, 62, 106–115.

[6] Rueda-Larraz, L.; Fernández-d'Arlas, B.; Tercjak, A.; Ribes, A.; Mondragon, I.; Eceiza, A. Synthesis and microstructure-mechanical property relationships of segmented polyurethanes based on a PCL-PTHF-PCL block copolymer as soft segment. Eur. Polym. J. **2009**, 45, 2096–2109.

[7] Dworakowska, S.; Bogdal, D.; Prociak, A. Microwave-assisted synthesis of polyols from rapeseed oil and properties of flexible polyurethane foams. Polymers **2012**, 4, 1462–1477.

[8] Lligadas, G.; Ronda, J. C.; Galià, M.; Cádiz, V. Plant oils as platform chemicals for polyurethane synthesis: current state-of-the-art. Biomacromolecules **2010**, 11, 2825–2835.

[9] Hojabri, L.; Kong, X.; Narine, S. S. Fatty acid-derived diisocyanate and biobased polyurethane produced from vegetable oil: synthesis, polymerization, and characterization. Biomacromolecules **2009**, 10, 884–891.

[10] Dworakowska, S.; Bogdał, D.; Zaccheria, F.; Ravasio, N. The role of catalysis in the synthesis of polyurethane foams based on renewable raw materials. Catal. Today **2014**, 223, 148–156.

[11] Zhang, C.; Madbouly, S. A.; Kessler, M. R. Biobased polyurethanes prepared from different vegetable oils. ACS Appl. Mater. Interfaces **2015**, 7, 1226–1233.

[12] Corcuera, M. A.; Rueda, L.; Fernandez-d'Arlas, B.; Arbelaiz, A.; Marieta, C.; Mondragon, I.; Eceiza, A. Microstructure and properties of polyurethanes derived from castor oil. Polym. Degrad. Stab. **2010**, 95, 2175–2184.

[13] Ugarte, L.; Fernández-d'Arlas, B.; Valea, A.; González, M. L.; Corcuera, M. A.; Eceiza, A. Morphology-properties relationship in high-renewable content polyurethanes. Polym. Eng. Sci. **2014**, 54, 2282–2291.

[14] Calvo-Correas, T.; Mosiewicki, M.A.; Corcuera, M. A.; Eceiza, A.; Aranguren, M. I. Linseed oil-based polyurethane rigid foams: synthesis and characterization. J. Renew. Mater. **2015**, 3, 3–13.

[15] Corcuera, M. A.; Saralegi, A.; Fernandez-d'Arlas, B.; Mondragon, I.; Eceiza, A. Shape memory polyurethanes based on polyols derived from renewable resources. Macromol. Symp. **2012**, 321-322, 197–201.

[16] Ugarte, L.; Saralegi, A.; Fernández, R.; Martín, L.; Corcuera, M. A.; Eceiza, A. Flexible polyurethane foams based on 100% renewably sourced polyols. Ind. Crops Prod. **2014**,

62, 545–551.

[17] Wang, Z.; Yu, L.; Ding, M.; Tan, H.; Li, J.; Fu, Q. Preparation and rapid degradation of nontoxic biodegradable polyurethanes based on poly(lactic acid)-poly(ethylene glycol)-poly(lactic acid) and L-lysine diisocyanate. Polym. Chem. **2011**, 2, 601–607.

[18] Yamamoto, N.; Nakayama, A.; Oshima, M.; Kawasaki, N.; Aiba, S. Enzymatic hydrolysis of lysine diisocyanate based polyurethanes and segmented polyurethane ureas by various proteases. React. Funct. Polym. **2007**, 67, 1338–1345.

[19] Skarja, G. A.; Woodhouse, K. A. Structure-property relationships of degradable polyurethane elastomers containing an amino acid-based chain extender. J. Appl. Polym. Sci. **2000**, 75, 1522–1534.

[20] Guelcher, S. A.; Gallagher, K. M.; Didier, J. E.; Klinedinst, D. B.; Doctor, J. S.; Goldstein, A. S.; Wilkes, G. L.; Beckman, E. J.; Hollinger, J. O. Synthesis of biocompatible segmented polyurethanes from aliphatic diisocyanates and diurea diol chain extenders. Acta Biomater. **2005**, 1, 471–484.

[21] Charlon, M.; Heinrich, B.; Matter, Y.; Couzigné, E.; Donnio, B.; Avérous, L. Synthesis, structure and properties of fully biobased thermoplastic polyurethanes, obtained from a diisocyanate based on modified dimer fatty acids, and different renewable diols. Eur. Polym. J. **2014**, 61, 197–205.

[22] Li, Y.; Noordover, B. A. J.; van Benthem, R. A. T. M.; Koning, C. E. Property profile of poly(urethane urea) dispersions containing dimer fatty acid-, sugar- and amino acid-based building blocks. Eur. Polym. J. **2014**, 59, 8–18.

[23] Li, Y.; Noordover, B. A. J.; van Benthem, R. A. T. M.; Koning, C. E. Chain extension of dimer fatty acid- and sugar-based polyurethanes in aqueous dispersions, Eur. Polym. J. **2014**, 52, 12–22.

[24] Calvo-Correas, T.; Santamaria-Echart, A.; Saralegi, A.; Martin, L.; Valea, Á.; Corcuera, M. A.; Eceiza, A. Thermally-responsive biopolyurethanes from a biobased diisocyanate. Eur. Polym. J. **2015**, 70, 173–185.

[25] Palmese, G. R.; McCullough, R. L. Effect of epoxy-amine stoichiometry on cured resin material properties. J. Appl. Polym. Sci. **1992**, 46, 1863–1873.

[26] Chenal, J. M.; Chazeau, L.; Guy, L.; Bomal, Y.; Gauthier, C. Molecular weight between physical entanglements in natural rubber: a critical parameter during strain-induced crystallization. Polymer **2007**, 48, 1042–1046.

[27] Bueno-Ferrer, C.; Hablot, E.; Perrin-Sarazin, F.; Garrigós, M. C.; Jiménez, A.; Averous,

L. Structure and morphology of new bio-based thermoplastic polyurethanes obtained from dimeric fatty acids. Macromol. Mater. Eng. **2012**, 297, 777–784.

[28] Fernández-d'Arlas, B.; Ramos, J. A.; Saralegi, A.; Corcuera, M.; Mondragon, I.; Eceiza, A. Molecular engineering of elastic and strong supertough polyurethanes. Macromolecules **2012**, 45, 3436–3443.

[29] Santamaría-Echart, A.; Arbelaiz, A.; Saralegi, A.; Fernández-d'Arlas, B.; Eceiza, A.; Corcuera, M. A. Relationship between reagents molar ratio and dispersion stability and film properties of waterborne polyurethanes. Colloids Surfaces A Physicochem. Eng. Asp. **2015**, 482, 554–561.

[30] Wu, X. L.; Kang, S. F.; Xu, X. J.; Xiao, F.; Ge, X. L. Effect of the crosslinking density and programming temperature on the shape fixity and shape recovery in epoxy-anhydride shape-memory polymers. J. Appl. Polym. Sci. **2014**, 131, 40559.

[31] Kaur, I.; Ray, P. Broader spectrum: examples. In *Polymer graffting and crosslinking*; Bhattacharya, A.; Rawlins, J.; Ray, P., Eds.; John Wiley & Sons: Hoboken, USA, **2008**.

[32] Ratna, D.; Karger-Kocsis, J. Recent advances in shape memory polymers and composites: a review. J. Mater. Sci. **2008**, 43, 254–269.

[33] Calvo-Correas, T.; Gabilondo, N.; Alonso-Varona, A.; Palomares, T.; Corcuera, M. A.; Eceiza, A. Shape-memory properties of crosslinked biobased polyurethanes. Eur. Polym. J. **2016**, 78, 253–263.

[34] E. Cognet-Georjon, F. Mechin, J.P. Pascault, New Polyurethanes Based on Diphenylmethane Diisocyanate and 1,4/3,6-Dianhydrosorbitol .1. Model Kinetic-Studies and Characterization of the Hard Segment, Macromol. Chem. Phys. 196 (1995) 3733–3751. doi:10.1002/macp.1995.021961125.

[35] E. Cognet-Georjon, F. Mechin, J.P. Pascault, New polyurethanes based on 4,4'-diphenylmethane diisocyanate and 1,4:3,6 dianhydrosorbitol .2. Synthesis and properties of segmented polyurethane elastomers, Macromol. Chem. Phys. 197 (1996) 3593–3612. doi:10.1002/macp.1996.021971109.

[36] Koberstein, J. T.; Stein, R. S. Small-angle X-ray scattering studies of microdomain structure in segmented polyurethane elastomers. J. Polym. Sci. Part B Polym. Phys. **1983**, 21, 1439–1472.

[37] Chen, Z. S.; Yang, W. P.; Macosko, C. W. Polymer synthesis and properties as a function of hard segment content. Rubber Chem. Technol. **1988**, 61, 86–99.

[38] Saralegi, A.; Etxeberria, A.; Fernández-D'Arlas, B.; Mondragon, I.; Eceiza, A.; Corcuera,

M. A. Effect of H_{12}MDI isomer composition on mechanical and physico-chemical properties of polyurethanes based on amorphous and semicrystalline soft segments, Polym. Bull. **2013**, 70, 2193–2210.

[39] Hojabri, L.; Kong, X.; Narine, S. S.Functional thermoplastics from linear diols and diisocyanates produced entirely from renewable lipid sources. Biomacromolecules **2010**, 11, 911–918.

[40] Sirkecioglu, A.; Mutlu, H. B.; Citak, C.; Koc, A.; Güner, F. S. Physical and surface properties of polyurethane hydrogels in relation with their chemical structure. Polym. Eng. Sci. **2014**, 54, 1182–1191.

[41] Oprea, S. The effect of chain extenders structure on properties of new polyurethane elastomers, Polym. Bull. **2010**, 65, 753–766.

FIGURES LIST

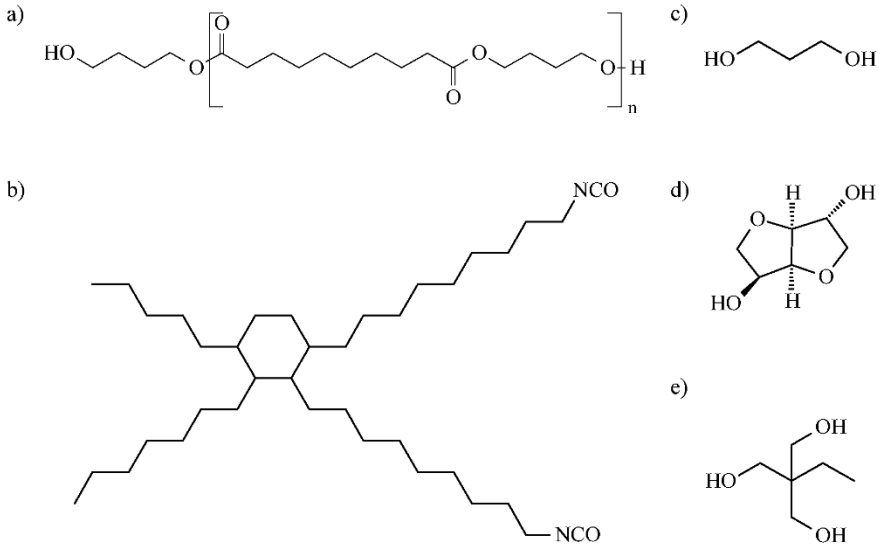

Figure 1. Chemical structure of a) macrodiol, b) DDI, c) PD, d) DAS and e) TMP.

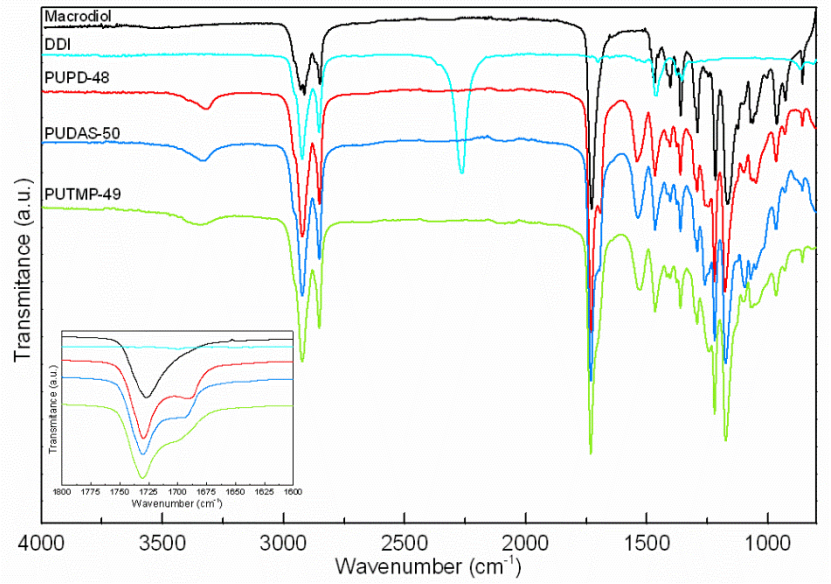

Figure 2. FTIR spectra of macrodiol, DDI and the synthesized biobased polyurethanes with PD, DAS and TMP. Inset: carbonyl group stretching region.

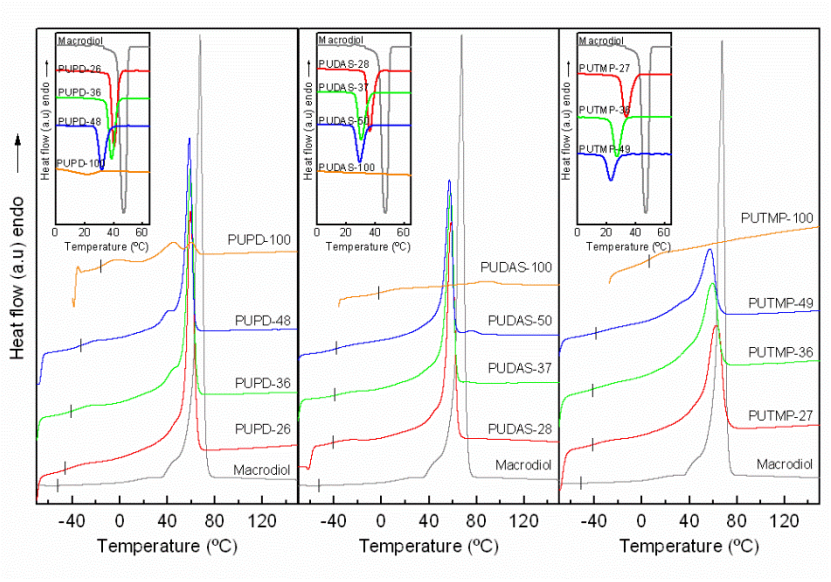

Figure 3. Heating and cooling (inset) DSC thermograms of the synthesized biobased polyurethanes with PD (left), DAS (center) and TMP (right) together with macrodiol and neat DDI/chain extender or crosslinker.

a)

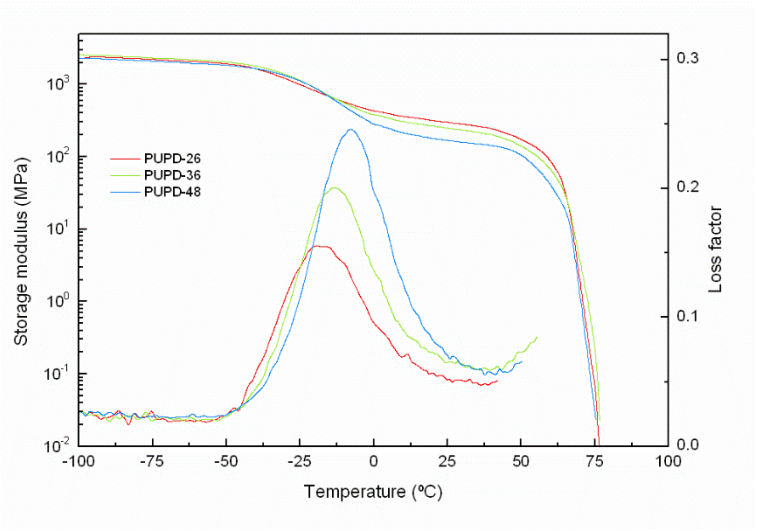

b)

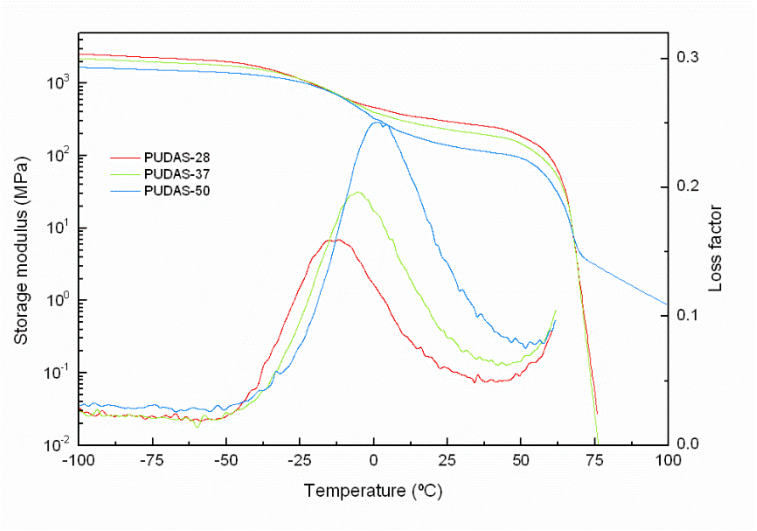

c)

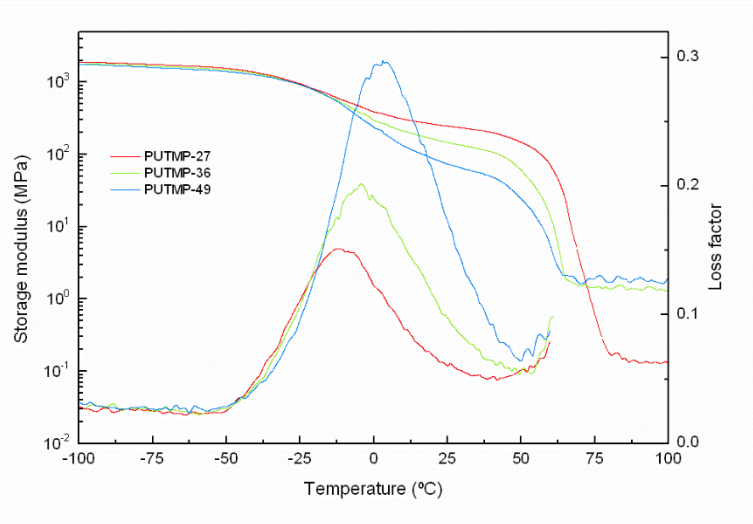

Figure 4. Storage modulus and loss factor of the synthesized biobased polyurethanes with a) PD, b) DAS and c) TMP.

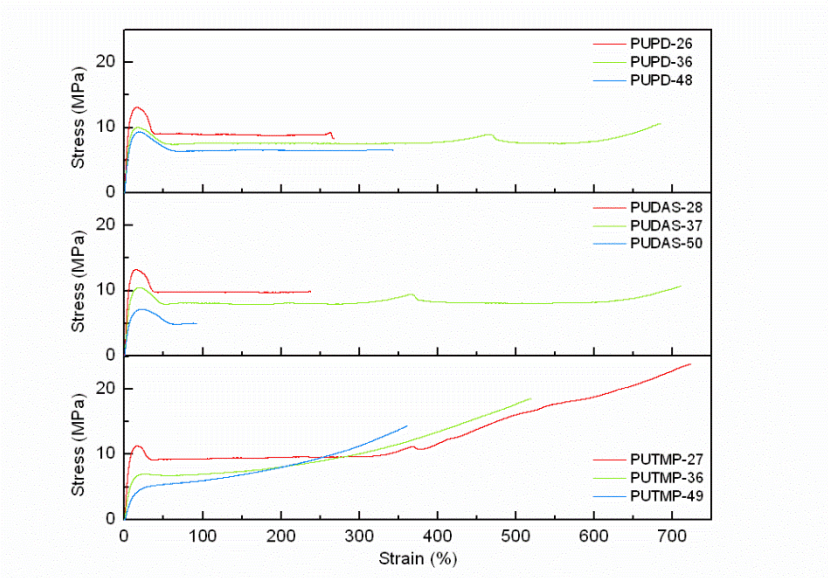

Figure 5. Strain-stress curves of the synthesized biobased polyurethanes.

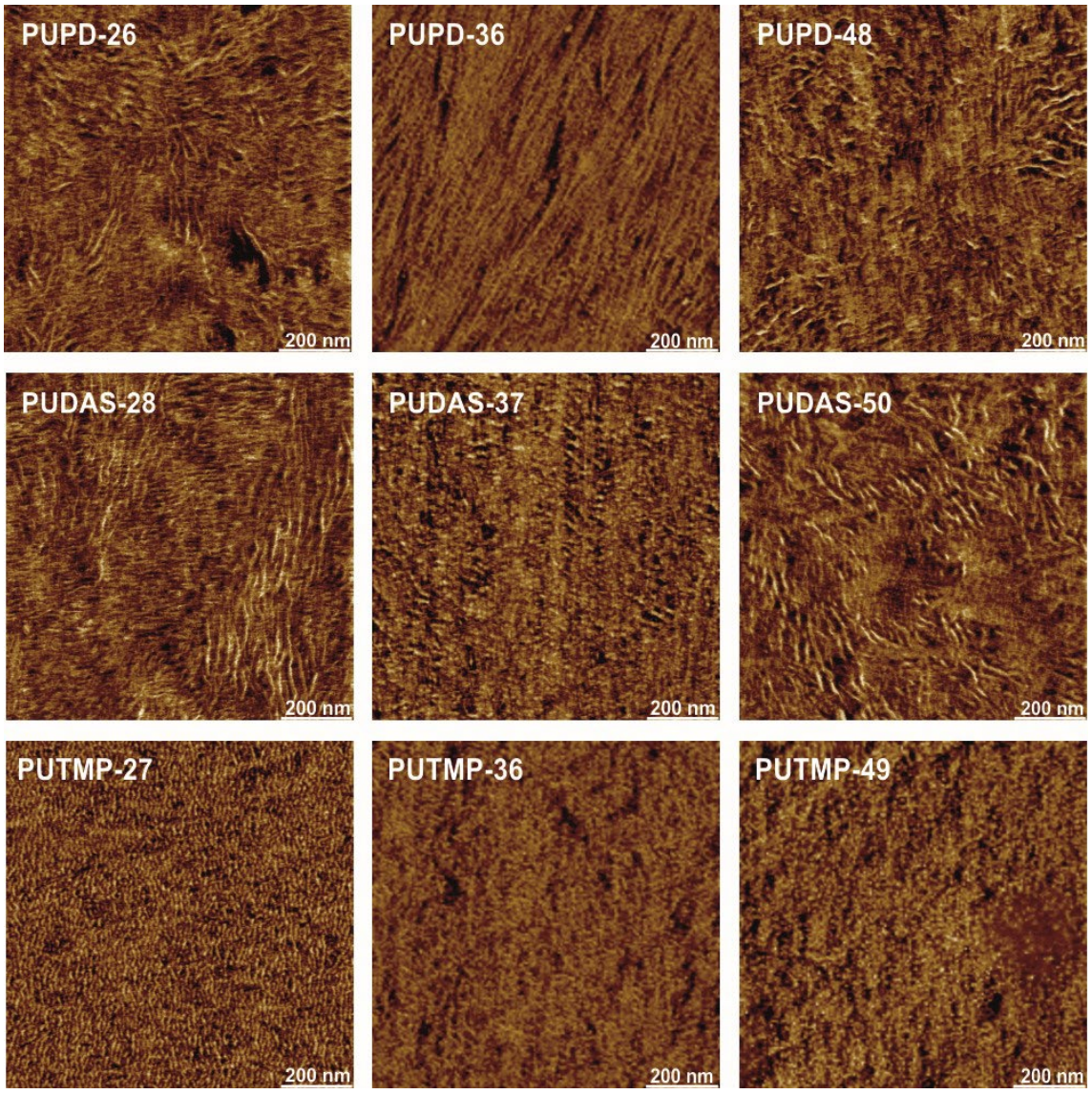

Figure 6. Phase AFM images of the synthesized biobased polyurethanes. Scan size: 1 x 1 μm^2.

TABLE LIST

Table 1. Weight average molecular weight, polydispersity index, crosslink density and average molecular weight between crosslinks of the synthesized biobased polyurethanes

Designation	Biobased carbon content (%)	$\bar{M}_w$ (g mol^{-1})	PI	ν_e (mol cm^{-3})	$\bar{M}_c$ (g mol^{-1})
PUPD-26	80	78000	2.4		
PUPD-36	83	75000	2.8		
PUPD-48	86	74000	3.0		
PUPD-100	98				
PUDAS-28	80	87000	2.4		
PUDAS-37	83	80000	2.4		
PUDAS-50	86	47000	2.2		
PUDAS-100	98				
PUTMP-27	78			17	69000
PUTMP-36	79			157	7600
PUTMP-49	80			195	6100
PUTMP-100	84				

Table 2. Thermal transition values of macrodiol and the synthesized biobased polyurethanes

Sample	T_g (ºC)		T_m (ºC)	ΔH_m (J/g)	T_c (ºC)	ΔH_c (J/g)
	DSC	DMA				
Macrodiol	-52.0		70.0	142.0	46.3	-93.1
PUPD-26	-45.6	-17.9	59.1	73.7*	40.5	-69.5
PUPD-36	-40.2	-13.3	45.79 / 59.0	67.7*	38.7	-64.5
PUPD-48	-35.5	-8.0	41.35 / 58.3	56.0*	31.9	-50.5
PUPD-100	-14.4		44.9 / 60.1	13.8	21.2	-8.2
PUDAS-28	-41.1	-13.5	58.6	76.7	36.4	-63.9
PUDAS-37	-39.7	-5.5	57.9	60.6	30.5	-57.1
PUDAS-50	-38.5	1.6	57.2 / 75.9	45.4 / 0.8	29.5	-43.6
PUDAS-100	-1.1		89.6	5.3	-	-
PUTMP-27	-39.4	-13.2	62.3	63.2	33.6	-60.2
PUTMP-36	-37.2	-3.4	59.4	52.6	27.2	-50.6
PUTMP-49	-37.7	3.1	57.3	43.0	23.0	-37.1
PUTMP-100	9.3		-	-	-	-

* ΔHm of macrodiol and DDI/PD are encompassed

Table 3. Mechanical properties of the synthesized biobased polyurethanes

Sample	E (MPa)	σ (MPa)	ε (%)	Shore D
PUPD-26	242.86 ± 15.78	13.66 ± 0.73	271.66 ± 27.80	55.7 ± 0.8
PUPD-36	167.27 ± 7.97	10.76 ± 1.05	690.58 ± 9.23	51.4 ± 0.6
PUPD-48	135.39 ± 5.33	9.65 ± 0.37	345.69 ± 18.13	50.0 ± 0.7
PUDAS-28	226.15 ± 8.56	12.95 ± 0.63	262.33 ± 28.93	57.3 ± 0.5
PUDAS-37	150.34 ± 5.60	10.87 ± 0.37	714.81 ± 6.07	51.0 ± 0.7
PUDAS-50	106.90 ± 2.15	7.28 ± 0.10	87.41± 8.26	55.2 ± 0.6
PUTMP-27	163.40 ± 8.29	24.41 ± 1.85	760.31 ± 33.30	57.2 ± 0.5
PUTMP-36	81.94 ± 4.80	15.84 ± 1.94	514.45 ± 5.93	55.5 ± 0.9
PUTMP-49	37.26 ± 3.62	13.87 ± 1.71	363.53 ± 22.55	50.4 ± 0.9

Table 4. Contact angle and surface tension values of synthesized biobased polyurethanes.

Sample	Contact angle (º)	Surface tension (mN m^{-1})
PUPD-26	88.14 ± 0.63	19.40
PUPD-36	93.80 ± 1.22	15.87
PUPD-48	100.21 ± 1.55	12.32
PUDAS-28	87.99 ± 0.89	19.50
PUDAS-37	90.42 ± 0.91	17.93
PUDAS-50	98.28 ± 0.86	13.33
PUTMP-27	99.96 ± 0.73	12.45
PUTMP-36	100.13 ± 0.84	12.36
PUTMP-49	101.76 ± 0.51	11.54